COBEM 2023 27TH INTERNATIONAL CONGRESS OF MECHANICAL ENGINEERING

ABCM Brazilian Society of Mechanical Sciences and Engineering
27th ABCM International Congress of Mechanical Engineering
December 04-08, 2023, Florianópolis-SC, Brazil

# COB-2023-2171
# NUMERICAL AND EXPERIMENTAL STUDY OF A PULSATION DAMPER: APPLICATION OF A HYPERELASTIC MODEL FOR UNIAXIAL TENSION

**Matheus Alves Lima**
**João Paulo Barbosa**
**Renato do Nascimento Siqueira**
Instituto Federal de Educação, Ciência e Tecnologia do Espírito Santo – campus São Mateus, Rodovia BR 101 Norte, Km 58, Bairro Litorâneo – CEP 29.932-540, São Mateus – ES.
matheus.matheusalveslima@gmail.com, jpbarbosa@ifes.edu.br, renatons@ifes.edu.br

**Bruno Venturini Loureiro**
**Michel de Oliveira dos Santos**
Universidade Federal do Espírito Santo, Av. Fernando Ferrari, 514 – Goiabeiras - CEP 29075-910, Vitória – ES.
bruno.loureiro@ufes.br, michel.santos@ifes.edu.br

**Daniel da Cunha Ribeiro**
Universidade Federal do Espírito Santo – campus São Mateus, Rodovia BR 101 Norte, Km 60, Bairro Litorâneo – CEP 29.932-540, São Mateus – ES.
gottfried.leibnitz@gmail.com

**Pedro Vitor Morbach Dixini**
Instituto Federal de Educação, Ciência e Tecnologia do Espírito Santo – campus Aracruz, Av. Morobá, 248 - Conj. Moroba – CEP 29192-733, Aracruz - ES.
pedrodixini@gmail.com

***Abstract.*** *Pulsation dampers (attenuators) are devices used to reduce pressure and flow pulsations in industrial pumping systems, seeking to improve efficiency and avoid problems such as mechanical vibrations and process instabilities. The objective of this work was to develop a three-dimensional computational model of fluid structure interaction (FSI) applied to the analysis of a rubber pulsation damper, validating the results obtained through experimental tests with a pumping system with pulsating flow. Numerical analysis was performed using the finite element method, implemented in the Ansys tool, with the third-order hyperelastic Yeoh model, based on uniaxial tensile test data. The computational results were compared with the experimental ones, and the third-order Yeoh model proved to be adequate, providing a good coincidence in the form of the maximum strain along the attenuator. However, there was greater homogeneity in the distribution of strain in the numerical tests compared to the experimental ones, possibly due to influences in the manufacturing process of the attenuators. The simulation proved to be satisfactory and promising for future analyzes of pulsation dampers with rubber materials.*

***Keywords:*** *Fluid structure interaction, computational fluid dynamics, pulsation damper, rubber*

## 1. INTRODUCTION

In the oil industry, to extract oil and natural gas efficiently, it is necessary to use lifting techniques that overcome high loads and adapt to the characteristics of the pumped fluid, such as high viscosity, being multiphase or containing particulates. Generally, positive displacement pumps are employed to meet these demands. However, due to the operating conditions, the pumping system may present an intermittent flow, known as pulsating flow, which generates significant pressure oscillations, affecting the operation, the useful life of the installations and industrial safety. To mitigate this problem, installing flow attenuators close to the pump outlet is an effective solution. Pulsation dampers are devices that seek to maintain a stable flow in the pumping system, and the in-line type, made of flexible viscoelastic elastomer tube, are able to accumulate flow energy in times of high flow and return it in periods of low flow, reducing pressure and flow oscillations and attenuating the flow (Wachel and Price, 1988; Henn, 2006; Xiaohui et al., 2015; Koegler et al., 2016; Geverini, 2017).

Rubbers, also known as hyperelastic materials, are widely used in various industrial applications due to their ability to withstand large deformations under small loads and maintain their original configuration after load removal. The mechanical and physical-chemical properties of rubbers depend on the components used in their formulation, as well as

on the processing parameters. These materials are viscoelastic, behaving simultaneously as elastic solids and viscous fluids. Their stress-strain behavior is highly non-linear, which makes the characterization of the elastic behavior of these materials fundamental for industrial applications with high vibration environments, wear or chemical and/or thermal degradation. Although there are pulsation dampers available on the market, the literature does not describe functional relationships between the mechanical behavior of the materials used to manufacture them and the structural and dynamic characteristics that affect the efficiency of the process (Meyer et. al, 2006; Schaefer, 2010; Shazad et. al, 2015; Oliveira et. al, 2016; Zhao Dong Xu et. al, 2016).

In studies on the fluid-structure interaction, the flow boundaries are influenced by the movement of the structure itself. This type of interaction consists of analyzing how the moving fluid affects the structure and how the structure's response influences the fluid. In the context of pulsation dampers applied in industrial systems, research on fluid-structure interaction is similar to studies in the area of hemodynamics, where blood flow in the cardiovascular system also presents periodic pulses that need to be controlled. During systole, when the heart contracts and pumps blood into the blood vessels, the arteries, which are composed of collagen, dilate temporarily to store the excess blood ejected. In diastole, the heart's relaxation phase, the artery wall contracts and returns to its original shape, converting potential energy into kinetic energy to boost blood flow. The analysis of these interactions is essential to understand the behavior of blood flow and design effective flow attenuators in industrial systems (Feijó, 2007; Cicigliano, 2010).

One of the ways to find improvements for processes and products without having an initial cost for prototyping and proof of concept is through computational tools, where behaviors can be simulated and effects understood in advance. Many researches with the aid of computational modeling using finite elements (FE) are carried out on hyperelastic materials, which shows the viability of models based on FE even when dealing with a material with non-linear behavior in relation to stress-strain. Numerical models that seek to approximate the mechanical properties of hyperelastic materials are found in the literature and used as a basis for understanding the behavior of these materials in engineering applications through computer simulations (Bradley, Chang and Mckenna, 2001; Palmieri et. al, 2009; Jamil, Irshad and Azmat, 2012). For analysis of studies in the area of fluid-structure interaction, numerical simulation allows estimating the displacement of the elastic tube wall according to input parameters for the flow and mechanical properties of the material (Cicigliano, 2010; Sedivy, Bursa and Fialova, 2019; Klas and Fiavolá, 2019). When it comes to looking for an approximate behavior of the stress-strain curve of a hyperelastic material subjected to uniaxial efforts, Yeoh's hyperelastic model presents results very close to those of an experimental test (Shahzad, et. al, 2015; Paula, Lalo and Greco, 2018).

In this context, validation of the pulsation damper behavior in numerical simulation through experimental tests is important for the development of models that describe the process more accurately and thus evolve this field of research. Thus, the objective of this work was to develop a three-dimensional computational model of fluid structure interaction (FSI) applied to the analysis of a rubber pulsation damper, validating the results obtained through experimental bench tests of a pumping system with pulsating flow. For this, a rubber composite attenuator was manufactured and tested, investigating the behavior of a pumping system and comparing it with its performance found by numerical simulations.

## 2. METHODOLOGY

### 2.1 Experimental procedures

The manufacturing process of the rubber tubes was carried out at the company Avutec (Araujo Vulcanização Técnica LTDA) in São Mateus - ES, using the NR/SBR rubber compound, Table 1. For this, the guidelines of the ASTM D3182-16 (2016) standard were followed to guarantee the quality of the production. The attenuators were manufactured through the compression molding process, which involved the development of a specific mold for their construction. Initially, the rubber compound passed through a mixing cylinder to form a continuous mat, and then fillers, plasticizers, antioxidants and other additives were added, Figure 1(a). Afterwards, the vulcanization ingredients, such as sulfur, TMTD and MBT accelerators, were introduced and the material was placed in the mold to start the vulcanization process. The rubber attenuator was subjected to a heated press at 180 ± 5°C for 5 minutes, Figure 1(b), measured in the center of the mold using a ZEM infrared thermometer at a distance of 15 cm from the part, followed by cooling in water at room temperature for another 10 minutes. After vulcanizing the attenuator, a finish was made to remove excess material. Thus, the final dimensions of the manufactured attenuator were 225 mm in length (useful length in the hydraulic circuit of 150 mm), 23 mm in external diameter and 3 mm in thickness.

Table 1. Formulation used for the development of rubber attenuators.

| Component | Material | Amount (phr) |
|---|---|---|
| Elastomer | Natural rubber GEB -1 (44.4%) e SBR 1712 (55.6%) | 100.00 |
| Reinforcement charge | Calcium carbonate | 16.67 |
| Reinforcement charge | FEF 550 (carbon black) | 44.44 |
| Reinforcement charge | HAF 339 (carbon black) | 16.67 |
| Plasticizer | Plasticizing oil A | 15.56 |
| Processing assistant | Rosin Resin | 1.67 |
| Processing assistant | Asphalt | 2.22 |
| Processing assistant | SP 134 (Phenolic Resin) | 1.67 |
| Antioxidant | Vulcanox HS | 1.11 |
| Antioxidant | Dusantox 6 PPD | 1.11 |
| Activation Agent | Zinc Oxide | 4.44 |
| Activation Agent | Stiarin | 1.11 |
| Processing assistant | Panasec | 5.00 |
| Curing Agent | Sulfur | 1.50 |
| Vulcanization Accelerator | TMTD – Tioram | 0.43 |
| Vulcanization Accelerator | MBT | 1.07 |

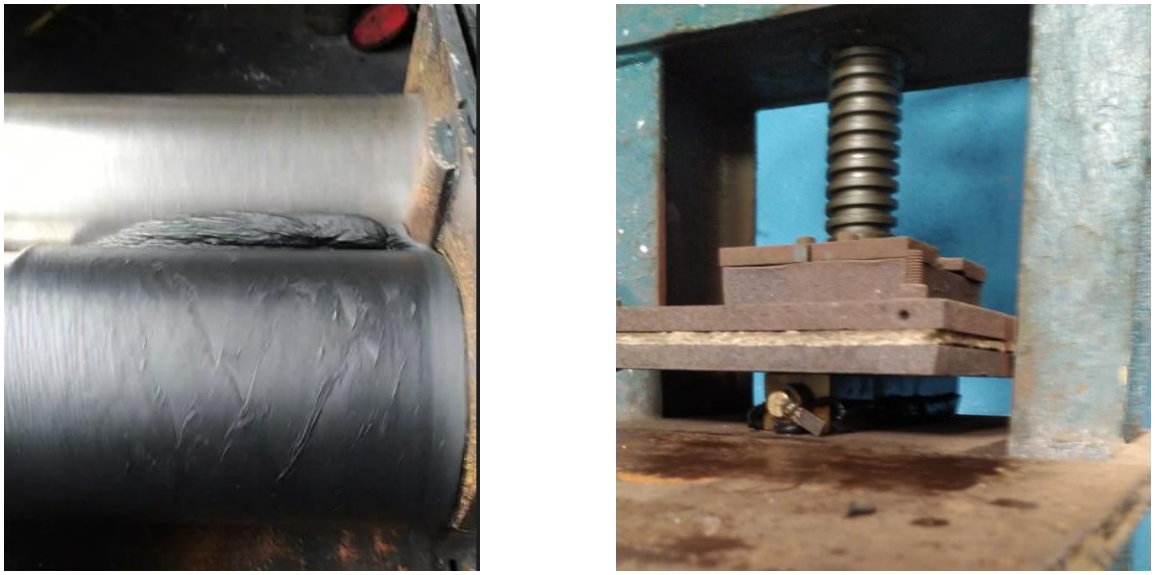

(a) (b)

Figure 1. Process of preparing a rubber attenuator. a) Mixing cylinder for mixing the components. b) Vulcanization under pressing.

The characterization of the material of the attenuators was through chemical analysis conducted using the Fourier Transform Infrared Spectroscopy (FTIR) technique, following the guidelines of the ASTM D2702-05 (2016) standard. The equipment used was the Agilent Cary 630 FTIR spectrophotometer, which has a high spectral resolution of 2 $cm^{-1}$ and precision of 0.05 $cm^{-1}$, covering a spectral range from 4000 to 650 $cm^{-1}$. For the analysis of high absorption samples, such as rubbers, the Total Attenuated Reflection (ATR) accessory with diamond crystal was used. The curves resulting from the test were generated using Essential FTIR® and Origin® software.

To survey the stress-strain curve, a tensile test was performed according to the ASTM D412-16 (2016) standard, using specimens removed from the attenuators. For this, the samples were cut in the transverse direction so that they were pulled during the test in the direction in which the main deformations occur during a pulsating flow test. To carry out the test, the Universal Testing Machine model WDW 200-E was used, equipped with a 1kN load cell and a displacement speed of the claws of 50 mm/min, maintaining the ambient temperature.

The performance of the rubber tube in the flow attenuation process was evaluated through tests on an experimental bench composed of a hydraulic circuit with a positive displacement pump, a reservoir, rigid stainless steel pipes for the fluid transport and a modular section for mounting the attenuators. Bench instrumentation includes pressure gauges upstream and downstream of the modular section, as well as a flow sensor positioned at the bottom of the bench, past the modular section, for data collection. The tests were conducted at room temperature, using water as the operating fluid, a

pump stroke opening of 35% and a frequency of 0.42 Hz, with an average pressure of the upper peak of the system around 0.82 bar for a rigid component. The first experiment was carried out with rigid polyvinyl chloride (PVC) tubing, and then the section was replaced by an attenuator made of rubber. The data capture system was configured to save the data of the first 400 seconds of each test, guaranteeing the stability of the parameters during the analysis, with a sampling time of 80 ms.

The behavior of the attenuator during experimental tests in the hydraulic circuit can be captured using a high-resolution camera. To capture the images, a PFV4 camera was positioned at a distance of 43 cm from the attenuator, while the light source was at a distance of 89 cm. The camera adjustment parameters were a Frame rate of 250 fps, Shutter speed of 1/7000 s. The structure needed to capture the images can be seen in Figure 2.

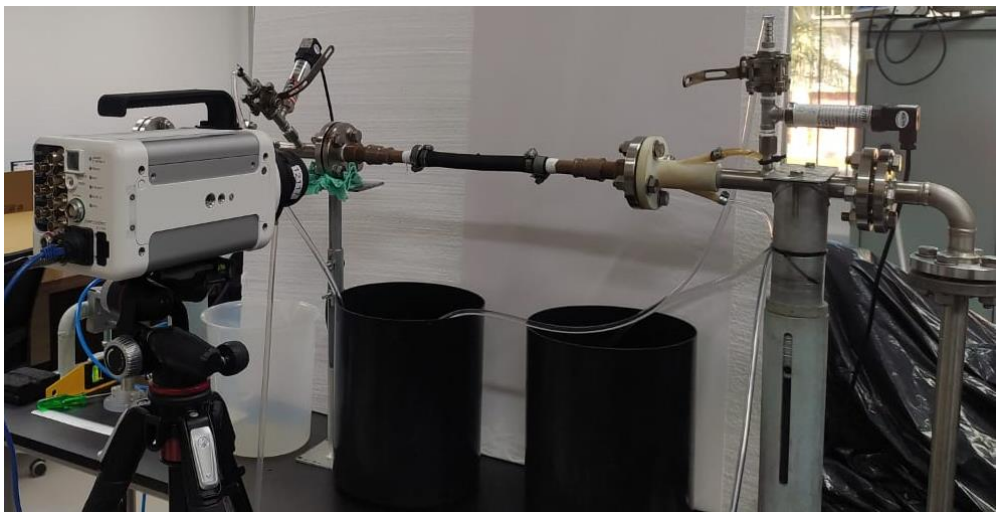

Figure 2. Assembly for experimental testing in the hydraulic circuit.

With the captured images, a comparative analysis was carried out between the diameter of the attenuator when it was at rest and when it was at its maximum deformation, in order to obtain the variation in radial deformation. The captured images were processed using ImageJ software. Each attenuator image was subdivided into 21 segments, considered rings, as illustrated in Figure 3, and the diameters were measured in pixel units for each ring. To convert these measurements to centimeters, an additional image of the attenuator, containing a millimeter ruler, was captured in the same position, providing a rough estimate of 60 pixels per centimeter.

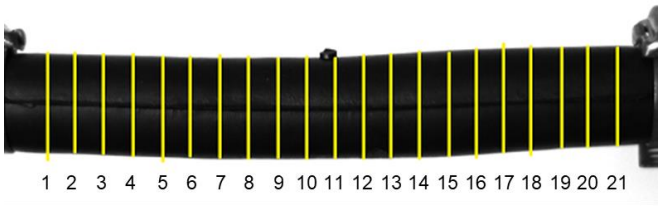


Figure 3. Illustration of the positioning of the rings to determine the radial deformation.

### 2.2 Computer simulation

The geometry of the investigated tubular attenuator, Figure 4, with an internal diameter of 17 mm, a wall thickness of 3 mm and a length of 150 mm, was constructed using the DesingModeler tool, integrated into the Ansys Workbench 2023 R1 package. For the numerical simulation of the behavior of the tubular attenuator, the finite element method implemented in the Ansys Mechanical tool, also integrated into the Ansys Workbench 2023 R1 platform, was used. In this analysis environment, the complex geometry of the device was discretized by generating a mesh composed of 23422 tetrahedral elements and 41596 nodes. Mesh quality was previously tested to ensure accuracy and reliability of results, with acceptable speed for obtaining results.

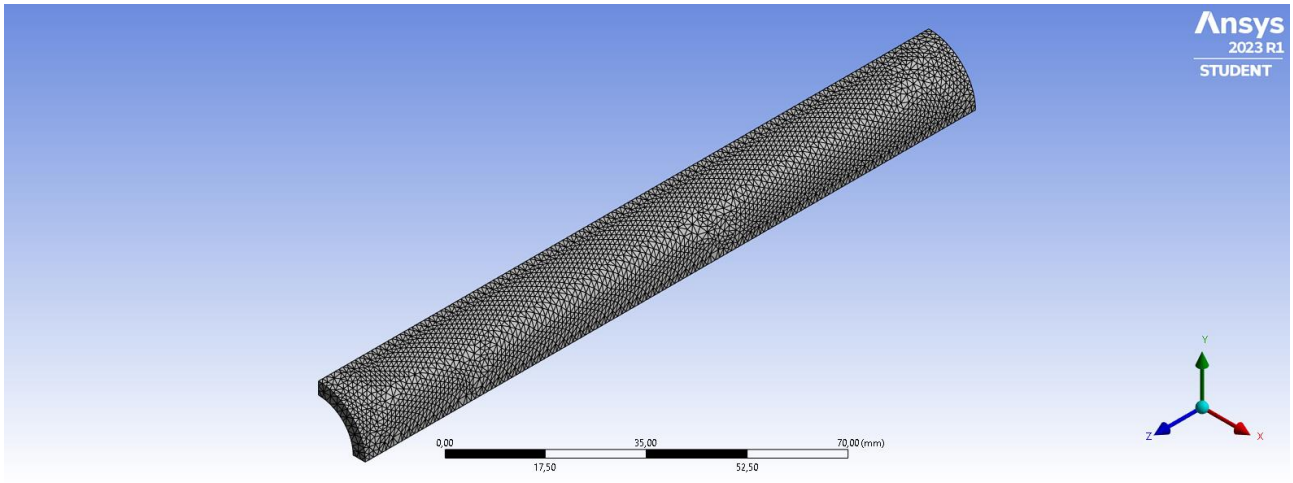


Figure 4. Model generated for the attenuator using the Ansys software.

To represent the appropriate constitutive relationship for the material, the third-order Yeoh hyperelastic material model was implemented from the tensile test data. This constitutive model is based on a polynomial expansion of the strain energy with respect to the Green-Lagrange strain invariants. The model formulation is represented by the following equation:

$$Ed = C1(I1 - 3) + C2(I1 - 3)^2 + C2(I1 - 3)^3, \quad (1)$$

where Ed is the strain energy per unit volume, C1, C2 and C3 are the material parameters that were determined from the least squares method on the experimental data and I1 is the first invariant of the Green-Lagrange strain tensor.

In order to simulate the operating conditions of the tubular attenuator, boundary conditions were applied at the ends of the device, in which they were considered completely fixed. These conditions represent a practical scenario where the attenuator is rigidly connected to its surrounding structure. To analyze the behavior of the tubular attenuator under different internal pressures, the pressure applied to the internal wall of the device was varied from 1.250 kPa to 100 kPa (1 bar), with increments of 1250 Pa. This variation allowed obtaining 80 sets of results, in which the radial displacement, the stress distribution and the deformation of the internal wall of the attenuator were recorded.

## 3. RESULTS AND DISCUSSION

Through the FTIR test, it was possible to characterize the rubber compound used in the development of the flow attenuator. After obtaining the data from the spectrophotometer, a smoothing of the signal was performed, followed by the application of the limits of interest as shown in Figure 5. Then, a comparative analysis was conducted, comparing the absorption peaks obtained with the diagnosis established by ASTM D3677 (2019). All absorption bands for SBR and NR materials presented in the standard could be identified in the test. Regarding the intensity of the peaks, the bands referring to NR rubber were coherent with what was expected, while for SBR the peaks were in the same proportion, except for the band at 1490 $cm^{-1}$, which presented a lower intensity than expected.

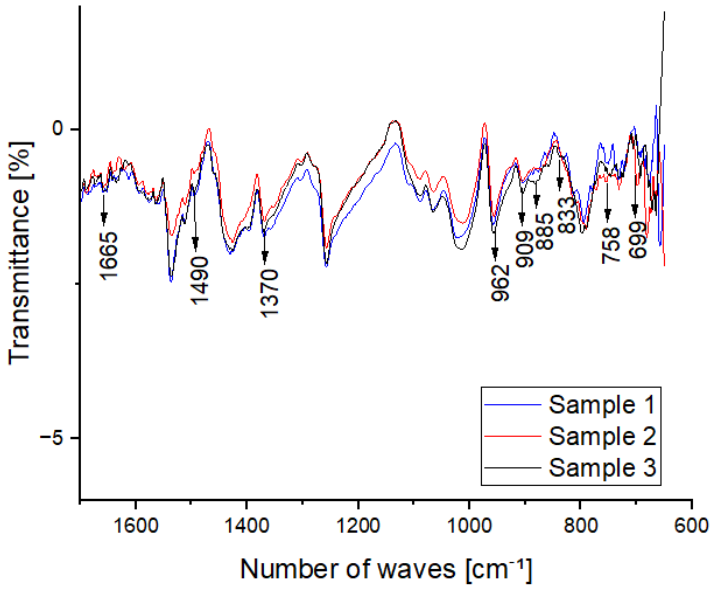


Figure 5. FTIR test results.

After carrying out the tensile tests, it was possible to obtain the mechanical properties of the rubber used and better understand its behavior as the material stretches. The results obtained were approximately 0.63 MPa for the modulus of elasticity at 100% elongation. The curve that illustrates the behavior is shown in Figure 6. The results obtained were used to feed the third-order Yeoh hyperelastic model that was used for the numerical simulation of the flow attenuator.

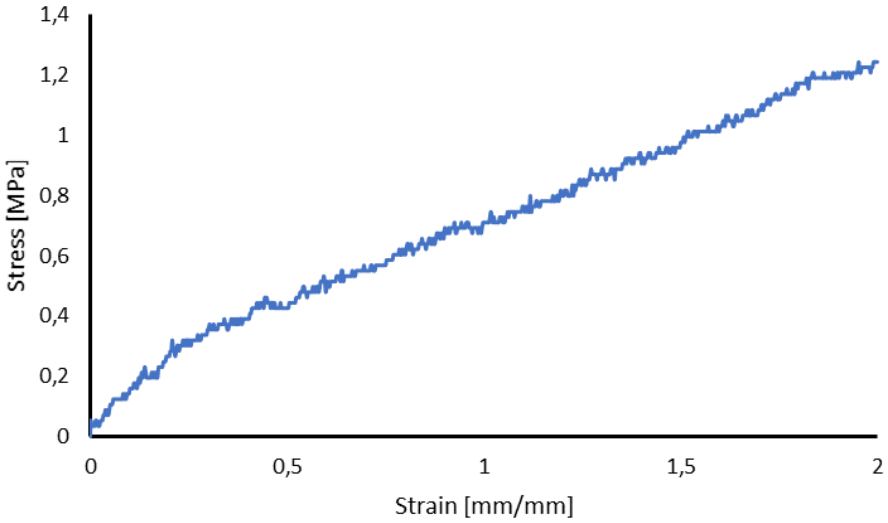


Figure 6. Uniaxial traction test results.

After collecting the experiment information, the downstream pressure data were processed to eliminate inconsistent data using Matlab software. These data provided information on the behavior of the fluid flow, before and after being attenuated, through the pressure sensors installed on the experimental bench. A curve showing the variation of pressure as a function of time was plotted, allowing the pulsating behavior of the fluid to be observed. In Figure 7, the blue curves represent the assembly with the rigid component (PVC), while the red curve represents the flexible tube (rubber attenuator). The data from the behavior of the rubber attenuator during the execution of the experiment were used to feed the input parameters of the numerical simulation by Ansys, as in the case of the pressure range of the system.

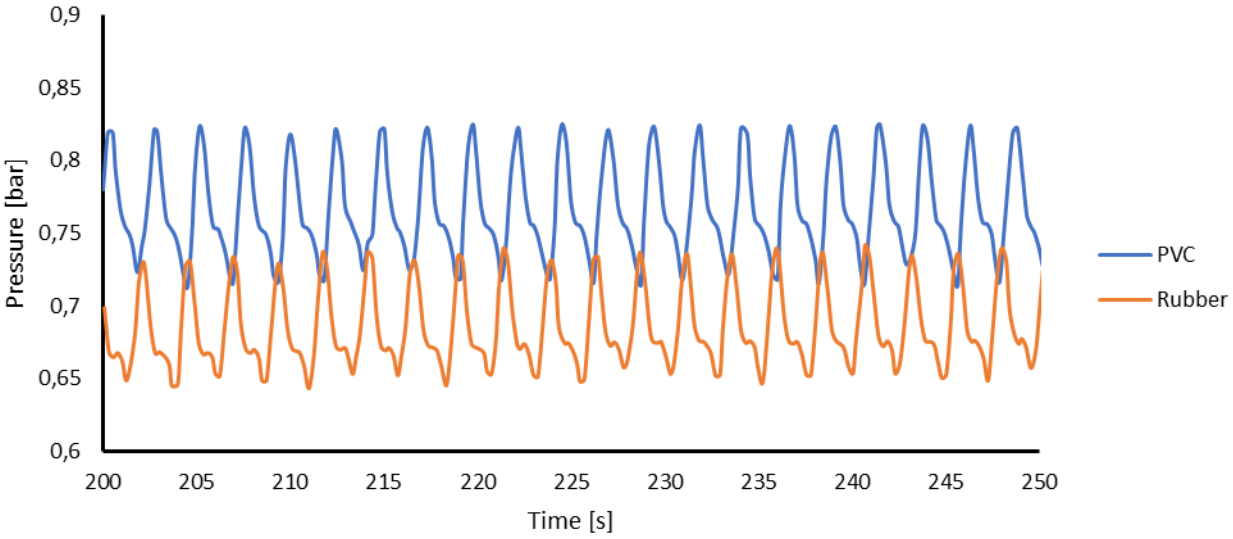


Figure 7. Attenuation test results.

To determine the attenuation of the fluid, a time range between 200 and 400 seconds was initially considered to eliminate the effects of transient behavior on the results. Then, the maximum and minimum pressure peaks were averaged, and the amplitude was calculated as the difference between these average values. The ratio between the pressure amplitudes of the rigid component and the rubber attenuator (AR) allowed to obtain an estimate for the attenuation of the fluid (Eq. (2)).

$$Attenuation\ (\%) = (1 - 1/AR).100 \tag{2}$$

As a result, a pulsating flow attenuation of 27.86% was obtained. This result indicates that the attenuator absorbed energy during high pressure pulses and returned it in moments of lower pulse, reducing the pressure amplitude compared to rigid PVC piping, which proves the influence of the viscoelastic properties of the material in the system.

Through the analysis of the images captured by the camera, it was possible to determine the area occupied by the attenuator and perform a subtraction between the image of the initial moment at rest and the moment in which the component presented the greatest deformation during the cycle, as shown in Figure 8. The result obtained was an area variation of 5.15 cm². By comparing the estimated radius of the attenuator using the image, it was possible to determine an average radial deformation value for the entire length of the attenuator of 1.47 mm. Variations in the radius were observed along the attenuator, as seen in Figure 8(c), showing a radial deformation of 1.33 mm near the central region and 1.83 mm in the adjacent part.

Figure 8. Photographs of the attenuators treated in binary color. a) Attenuator at rest. b) Pressurized attenuator with maximum deformation. c) Subtracted images.

Regarding the computational analysis, the result of the numerical simulation by Ansys was satisfactory. The set of results was used as a reference, in which the pressure applied to the wall of the tubular attenuator was the maximum pressure presented by the peaks identified in the experimental test in the hydraulic circuit, Figure 7, at approximately 0.73

bar. Thus, it was possible to compare the result of the photograph taken during the experiment containing the maximum deformation obtained, Figure 8 (b), with the deformation found in the numerical simulation, presented in Figure 9.

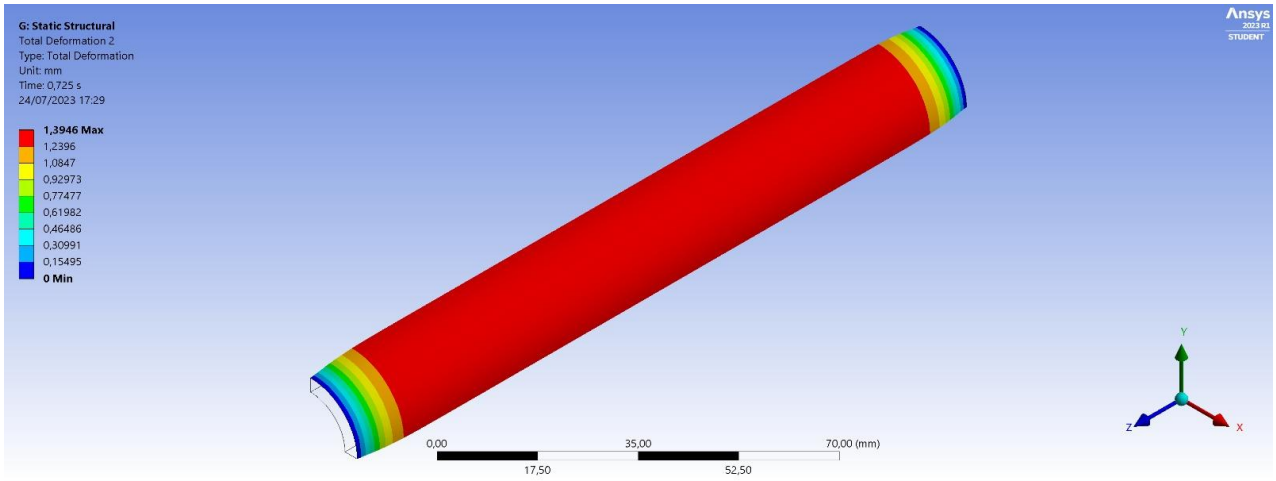


Figure 9. Deformation distribution through the mesh generated for the attenuator using the Ansys software.

From Figure 9, considering the useful length of the attenuator highlighted by the red color, it can be seen that the maximum radial deformation of the attenuator for the pressure used as reference was 1.39 mm, which is smaller but with a difference of 6.09 % in relation to the average radial deformation found with experimental tests. Therefore, in relation to radial deformation, the numerical result was very close to that found experimentally.

The distribution of the deformation of the mesh generated for the attenuator was constant along the entire length of the component, different from what happened in the experimental test, where some regions presented a slightly different deformation, which may be noticeable when observing the area variation of the subtracted image in Figure 8 (c). The difference in the behavior of the deformation distribution in the experimental test in relation to the numerical simulation may have occurred due to the impact of manufacturing the attenuator, at the time of preparation of the rubber compound, where the curing agents may not have been dispersed homogeneously throughout the mass, or during the vulcanization process, where a difference in time for demolding the component (in the order of seconds) may have interfered with the result. Such factors are not taken into account during a numerical simulation, where the geometry and material used do not present precision errors.

## 4. CONCLUSION

The experimental study successfully investigated the impact of a flexible component on the performance of the pumping system, effectively mitigating the pulsations caused by the positive displacement pump. The use of SBR rubber as a viscoelastic material was suitable for this purpose. The results obtained by the uniaxial tensile test were satisfactory for application in the third-order Yeoh hyperelastic model, in which the numerical simulation presented a mesh deformation very close to that obtained via image capture of the experimental test in a hydraulic circuit.

As future perspectives, the experimental tests in the hydraulic circuit will allow establishing relations between the geometric parameters of the developed elastic tube (radius, length and thickness) and the modulus of elasticity of the material with the data collected by the sensors that monitor the flow of the fluid. Additionally, dynamic-mechanical tests will be carried out for a more detailed analysis of the viscoelastic behavior of the pulsation damper, contributing to the interpretation of the phenomena observed throughout the experiments. In this way, it will be possible to better understand the impact of component geometry and material properties on pulsation damper performance.

## 5. ACKNOWLEDGEMENTS

To the Federal Institute of Espírito Santo, to the Federal University of Espírito Santo, to LabPetro (Cooperation term no. 0050.0022844.06.4) and to the company Avutec for their research support.

## 6. REFERENCES

American Society for Testing and Materials. "ASTM D2702 – 05: Standard Practice for Rubber Chemicals – Determination of Infrared Absorption Characteristics Manufacturing Industries". West Conshohocken: ASTM, 2016.

American Society for Testing and Materials. "ASTM D3182 – 16: Standard Practice for Rubber - Materials, Equipment, and Procedures for Mixing Standard Compounds and Preparing Standard Vulcanized Sheets". West Conshohocken: ASTM, 2016.

American Society for Testing and Materials. "ASTM D3677 – 10: Standard Test Methods for Rubber—Identification by Infrared Spectrophotometry". West Conshohocken: ASTM, 2019.

American Society for Testing and Materials. "ASTM D412 – 16: Standard Test Methods for Vulcanized Rubber and Thermoplastic Elastomers-Tension". West Conshohocken: ASTM, 2016.

Bradley, G. L.; Chang, P. C.; Mckenna, G. B., 2001. "Rubber modeling using uniaxial test data". *Journal of Applied Polymer Science*, v. 81, n. 4, p. 837-848.

Cicigliano, E. C. S., 2010. *Numerical analysis of fluid flow in elastic tubes (in Portuguese)*. Master's thesis, Paulista State University, Faculty of Engineering of Ilha Solteira, Ilha Solteira, Brazil.

Feijó, V., 2007. *Modeling blood flow in the abdominal aorta using fluid-structure interaction (in Portuguese)*. Master's thesis, Paulista State University, Faculty of Engineering of Ilha Solteira, Ilha Solteira, Brazil.

Gerevini, G. G., 2017. *Slug attenuation in oil lifting systems in offshore environments offshore (in Portuguese)*. Master's thesis, Federal University of Rio Grande do Sul, Porto Alegre, Brazil.

Henn, E. A. L., 2006. *Fluid Machines (in Portuguese)*. 2.ed. UFSM, Santa Maria, Brazil.

Jamil, M. Y.; Irshad, M. A.; Azmat, Z., 2012. "Characterization of hyperelastic (Rubber) material using uniaxial and biaxial tension tests". *Advanced Materials Research*, v. 570, p. 1-7.

Klas, R.; Fialová, S., 2019. "Pulse flow of liquid in flexible tube". *EPJ Web of Conferences*.

Koegler. A. F.; Haselmann, D.; Alt, N. S. A.; Schluecker, E., 2017. "Experimental characterization of a flow-throught pulsation damper regarding pressure pulsations and vibrations". *Chemical Engineering & Technology*, Weinheim, v.40, n.1, p.162-169.

Meyer, A. L. et al., 2006. "Evaluation of the Thermo-Mechanical Properties of Nitrile Rubber after Compatibility Testing in accordance with ASTM D 3455 (in Portuguese)". *Polímeros: Ciência e Tecnologia*, [S.l.], v. 16, n. 3, p. 230-234.

Oliveira, M. A. S. et al., 2016. "Influence of the vulcanization method on the mechanical properties and cross-link density of natural rubber (in Portuguese)". *Polímeros: Ciência e Tecnologia*, v. 26, p. 43-48.

Palmieri, G. et al., 2009. "Hyperelastic materials characterization by planar tension tests and full-field strain measurement". *In: Proceedings of the SEM Annual Conference*. Albuquerque: Society for Experimental Mechanics.

Paula, J. P. A. de., 2018. "Numerical modeling and experimental characterization of elastomers subjected to uniaxial stresses (in Portuguese)". *XIII SIMMEC*. Federal University of Espirito Santo, Vitória.

Schaefer, R. J., 2010. *Mechanical properties of rubber*. In: PIERSOL, A. G.; PAEZ, T. (Eds.). Harris' Shock and Vibration Handbook. 6. ed. [S.l.]: McGraw-Hill Companies Inc., p. 33.1-33.18.

Sedivy, D.; Bursa, J.; Fialová, S., 2019. "Experimental and numerical investigation of flow field in flexible tube". *29 th IAHR Symposium on Hidraulic Machinery and Systems*.

Shahzad, M.; Kamran, A.; Siddiqui, M. Z.; Farhan, M., 2015. "Mechanical Characterization and FE Modelling of a Hyperelastic Material". *Materials Research*, v. 18, n. 5, p. 918-924.

Wachel, J. C.; Price, S. M., 1988. "Understanding how pulsation accumulators work. Engineering Dynamics Incorporated". *American Society of Mechanical Engineers*, Petroleum Division, San Antonio, v. 14, p. 23-31.

Xiaohui, L.; Shuping, C.; Weijie, S.; Xiaofeng, H., 2015. "Analysis and design of a water pump with accumulators absorbing pressure pulsation in high-velocity water-jet propulsion system". *Journal of Marine Science and Technology*, v. 20, n. 3, p. 551–558.

Zhao Dong Xu, A. M.; Liao, Y. X.; Ge, T.; Xu, C., 2016. "Experimental and Theoretical Study of Viscoelastic Dampers with Different Matrix Rubbers", *Journal of Engineering Mechanics*, v. 142, n. 8.

## 7. RESPONSIBILITY NOTICE

The authors are the only responsible for the printed material included in this paper.